Attitude Control of UWE-4 for Orbit Correction during Formation Flying

IEPC-2015-493／ISTS-2015-b-493

By Siddharth DADHICH[1)], Philip BANGERT[2)] and Klaus SCHILLING[3)]

[1)] *Department of Computer Science, Electrical and Space Engineering, Luleå Technical University, Luleå, Sweden*
[2)] *Department of Computer Science VII: Robotics and Telematics, Würzburg University, Würzburg, Germany*
[3)] *Zentrum fuer Telematik, Gerbrunn, Germany*

UWE-4 is the fourth pico-satellite in the University of Wuerzburg Experimental satellite series. After the successful demonstration of on-board attitude determination and control with UWE-3 in 2013, the mission of UWE-4 is to validate electric propulsion technology for formation flying missions at the pico-satellite level of miniaturization. The challenge in this project is to demonstrate precise orbit and attitude control given the extremely limited resources available to the satellite. In this paper, attitude control of a CubeSat is studied and a simulation framework for the attitude and orbit control is presented. Different control philosophies are developed, compared and implemented to fly on-board UWE-4. The absence of a requirement for precise attitude control in the thrust axis together with having insufficient action in that axis has motivated the development of a quaternion based dynamic target attitude solution. This result helps in achieving precise 2D attitude control while also providing complete stabilization on the third axis. A non-linear controller has found to be advantageous over a linear controller for this particular problem of attitude control where frequent large angle manoeuvres are desired for changing the direction of thrust. Therefore, a sliding mode control has been implemented and evaluated for its performance.

Key Words: Attitude Control, Orbit Control, Sliding Mode Control, Innovative Small Satellite Mission

Nomenclature

I	:	Moment of inertia
ω_{ab}^{c}	:	Angular velocity of a with respect to b expressed in c
T_b^a	:	Transformation Matrix from a to b
q	:	Quaternions
μ_e	:	Earth's Gravitational Constant
a	:	Semi major axis
C_d	:	Drag coefficient
ρ	:	Density of air
υ	:	Velocity of satellite
A	:	Cross-section area for drag
L	:	Distance between center of gravity and center of pressure
$\vec{m}$	:	Magnetic moment
$\vec{B}$	:	Magnetic field
T	:	Torque demanded
F	:	Thrust produced
τ	:	Torque produced
Superscripts/Subscripts		
b	:	Body coordinate frame
o	:	Orbit coordinate frame
c	:	Control coordinate frame
s	:	Satellite
tor	:	Torquers
thr	:	Thrusters
dis	:	Disturbances
gg	:	Gravity gradient
aero	:	Aerodynamics

1. Introduction

The University of Wuerzburg, Germany, has established a roadmap towards formation flying pico-satellites.[1)] In this context three 1U CubeSats of the UWE (University Wuerzburg Experimental Satellite) series have been launched since 2005. With UWE-3[2,3)] being launched in Nov. 2013 real time attitude determination and control could be demonstrated[4)] which is to be extended towards orbit control with the next UWE satellite while preserving the one unit form factor. Suitable propulsion systems have been identified in the electric propulsion domain due to their high specific impulse[5)] and therefore only small amounts of propellants is sufficient. In cooperation with the University of the Federal Armed Forces Germany first concepts have been developed to mechanically integrate a propulsion system. At the same time, development of suitable control algorithms has been initiated at University of Wuerzburg taking into account the limitations of the physical system.

In the following contribution, first the attitude and orbit control simulation is introduced in sections 2 and 3. Attitude control algorithms dedicated to formation flying scenarios are presented in section 4 and their performance evaluation is reported in section 5. The contribution concludes with remarks on the suitability of these types of algorithms and actuators for attitude control in the scope of formation flying of CubeSats.

2. System Models

Since launching even the smallest satellite is very expensive, simulations become great tool to test attitude control algorithms. Therefore to do research on this subject, we developed a simulation environment which models the various parts of the

CubeSat and its environment.

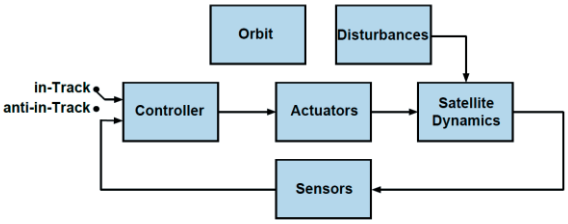

Fig. 1. The control block diagram

A block diagram of the attitude control simulation environment is shown in Fig. 1. Apart from the satellite's orbit (sec. 3) and the attitude controller (sec. 4), we discuss all other blocks from Fig. 1 in this section.

2.1. Coordinate frames

In this paper, four coordinate frames have been used as listed below

1. Earth centered inertial – ECI
2. Earth centered earth fixed - ECEF
3. Body coordinate frame – BCF
4. Orbit coordinate frame – OCF
5. Control coordinate frame – CCF

The ECI and ECEF frame are used as defined in 6). The definition of BCF frame follows its legacy from UWE-3. The BCF frame together with OCF and CCF frames are defined in Table 1. The BCF-Y, OCF-Z and CCF-Z complete the triad with the other two axes, respectively. The motivation behind choosing the CCF different from BCF is to be able make CCF and OCF to coincide for one of the two directions (anti-in-track and in-track) for simplified calculations in the control laws.

Table 1. Body Coordinate Frame.

Frame-axis	Direction
BCF-X	Opposite to the front access panel
BCF-Z	Towards Antennas
OCF-X	In the velocity direction
OCF-Y	Towards earth
CCF-X	In thruster mounting direction
CCF-Y	Opposite to the front access panel

2.2. Satellite dynamics

In this paper, the attitude of the satellite is defined as the angle between the orbit coordinate frame and the control coordinate frame. The attitude can be derived from the Euler equations presented in Eq. (1)

$$I_s \dot{\omega}_{bi}^c + \omega_{bi}^c \times I_s \omega_{bi}^c = \tau_{total}^c \tag{1.}$$

where the total torque experienced by the satellite is given as in Eq. (2)

$$\tau_{total}^c = \tau_{tor}^c + \tau_{thr}^c + \tau_{dis}^c \tag{2.}$$

Following the definition of attitude in this work, we need to obtain the angular velocity of CCF w.r.t. BCF as seen in OCF (ω_{bo}^c). When, $\omega_{bo}^c = [\omega_x \quad \omega_y \quad \omega_z]^T$ we can write the kinematic equation for satellite's attitude as in Eq. (3)

$$\dot{q} = \frac{1}{2}\begin{bmatrix} 0 & -\omega_x & -\omega_y & -\omega_z \\ \omega_x & 0 & \omega_z & -\omega_y \\ \omega_y & -\omega_z & 0 & \omega_x \\ \omega_z & \omega_y & -\omega_x & 0 \end{bmatrix} q \tag{3.}$$

In order to obtain ω_{bo}^c from the simulated gyroscope data, we also need Eqs. (4) and (5)

$$\omega_{bi}^c = \omega_{bo}^c + \omega_{oi}^c \tag{4.}$$

$$\omega_{oi}^c = T_c^o [0 \quad 0 \quad -\omega_o]^T \tag{5.}$$

where ω_o is the angular velocity of the OCF w.r.t to the ECI coordinate frame.

2.3. Sensors

The simulated noise free gyroscope data ($\widetilde{\omega}_{gyro}$) can be obtained from Eq. (6), where ω_{bi}^c comes from the solution of the Euler moment equation.

$$\omega_{bi}^c = T_c^b \widetilde{\omega}_{gyro} \tag{6.}$$

The magnetic field data is obtained from the standard IGRF[7] earth's magnetic field model. To simulate real sensor effects, the gyroscope and magnetometer values are augmented with white Gaussian noise according to the Eqs. (7) and (8)

$$\omega_{gyro} = \widetilde{\omega}_{gyro} + N_{WGN} \tag{7.}$$

$$B_{mag} = T_b^{ECEF} B_{ECEF} + N_{WGN} \tag{8.}$$

Since magnetic field models such as the standard IGRF gives the magnetic field in the ECEF frame, an appropriate transformation is also required to convert the magnetic field into BCF.

2.4. Actuators

Due to the technological limitations with the selected nano-thrusters i.e. VAT[8], it is assumed that the four thrusters cannot be ON simultaneously. Therefore, whenever a thruster is ON, it produces a force as well as a torque on the satellite.

It is impractical to run the simulation at the time scale of an individual thruster firings which is in the order of microseconds. Therefore, ON commands to the four thrusters are combined for one simulation step in the vector n_i which then represents the number of firings of the thruster subsystem. The force and torque by the thruster subsystem for one simulation step is then given by Eqs. (9) and (10)

$$F_{thr} = \sum_{i=1}^{n} -n_i f_i p_i T_0 \tag{9.}$$

$$\tau_{thr} = \sum_{i=1}^{n} -n_i (p_i \times f_i T_0) \tag{10.}$$

where p_i and f_i are the position vector and firing direction of i^{th} thruster respectively and T_0 is the average magnitude of the thrust. It is a known fact that T_0 will decay during the lifespan of the thrusters and that f_i will not be the same for every firing. Therefore, a life model for T_0 and a plume model for f_i has also been considered in the simulations.

The magnetic torquers produce a magnetic moment which interacts with the Earth's magnetic field to produce a torque on the satellite according to Eq. (11)

$$\tau_{tor} = \vec{m} \times \vec{B} \tag{11.}$$

Given a desired torque to be produced, the magnetic moment required from the torquers can be computer by Eq. (12)

$$\vec{m} = \frac{\vec{B} \times T_c}{|\vec{B}|^2} \quad (12.)$$

The magnetic torquers and the attitude determination system developed of the UWE satellites are presented in 9).

2.5. Disturbances

Apart from the effects produced by the actuators, several disturbances act on the satellite in its orbital motion. For a CubeSat at an altitude of ~500-600 km, the three main disturbance torques as presented in 10) are the gravity gradient torque Eq. (13), the aerodynamic drag torque Eq. (14) and the residual magnetic field torque given in Eq. (15).

$$\tau_{gg} = 3\frac{\mu_e}{a^3}(c_3 \times I_s c_3) \quad (13.)$$

$$\tau_{areo} = \frac{1}{2} C_d \rho v^2 AL \quad (14.)$$

$$\tau_{magnetic} = \vec{m}_{residual} \times \vec{B} \quad (15.)$$

Where c_3 is the third column in transformation matrix T_O^c and $\vec{m}_{residual}$ is the magnetic moment generated by the internal electronics of the satellite.

Given the size of a CubeSat, it is often observed that $\tau_{magnetic}$ dominates the disturbance torques. The disturbance torques from the solar radiation pressure and the third body perturbations can be neglected for CubeSats.[10)]

In this section, we presented the dynamic model of the satellite's attitude with sensors (that determine the attitude), actuators and disturbances (that effect the attitude). The parameters identified in the model are assigned to appropriate values based on the design and experiment data from the UWE-3 satellite.

3. Orbit Propagator

In order for the satellite to track its changes on the orbit due to thrust actuation a sophisticated orbit propagator on board is required. In fact, in the scope of autonomous formation flying satellites a ground independent orbit determination needs to be implemented. These two aspects are currently being addressed and the approach is presented in the following paragraphs.

3.1. SGP-4

The orbit propagator used on board the UWE-3 satellite is the well-known SGP-4 propagator which relies on regular TLE updates from ground. Achievable position determination accuracies heavily depend on the ground-based ranging algorithms put forward by NORAD and are in the order of several kilometers. The benefit of this propagator is its analytical form which renders computationally heavy integration algorithms on board the satellite unnecessary. This is especially important for very low power applications such as the UWE CubeSats where the ADCS consumes only 15-60 mW in nominal operation by employing a 16 bit low power processor.

Inherent to the algorithm is that changes in the orbit need to be measured by ground and are only then included in the most recent TLE. This process however is very slow with updates at most once or twice per day and unknown integration algorithms. Therefore, a real time orbit control is not possible with this approach.

3.2. Sensor based orbit determination

In order to also address the autonomous orbit determination an approach based on magnetometer and sun-sensor data fusion has been chosen. Information concerning the satellite's orbit obtained with these two sensor types comprise the magnetic field strength and the angle between the magnetic field and sun-vector. Currently, a Kalman filter based algorithm is being implemented that fuses this information and tracks the satellite's orbit in real time. First results of this approach are expected later this year.

The benefit of this method over a GPS based orbit determination clearly would be its low implication on the satellite system and a continuous operation due to its low power consumption. While a real time orbit determination is expected to be feasible with this approach, the expected accuracy is some orders of magnitude worse than GPS or TLE based techniques.

4. Attitude Control

The attitude control problem defined in this paper is motivated by the objective of orbit correction during formation flying in terms of adjustments to the orbit's semi-major axis. To make the maximum use of thrusters, the thrust vector should be aligned to the velocity vector to increase (in-track direction) or should be exactly opposite to the velocity vector to decrease (anti-in-track direction) the semi-major axis.

Since the accurate alignment of all three body axes with the OCF is not needed to meet this requirement, a precise 3 axes control is not a necessity. Nevertheless, spin stability in the CCF-X is desired to curb the possibility of nutation.

The interesting requirements from the attitude control problem demand to compute the reference attitude dynamically which is discussed in the next subsection.

4.1. Reference attitude

Assuming that the reference (target) attitude is represented by $q_T = [q_{T1} \quad q_{T2} \quad q_{T3} \quad q_{T4}]^T$ and the current attitude by $q = [q_1 \quad q_2 \quad q_3 \quad q_4]^T$, the error in attitude as given in 11) is:

$$q_E = \begin{bmatrix} q_{E1} \\ q_{E2} \\ q_{E3} \\ q_{E4} \end{bmatrix} = \begin{bmatrix} q_{T4} & q_{T3} & -q_{T2} & -q_{T1} \\ -q_{T3} & q_{T4} & q_{T1} & -q_{T2} \\ q_{T2} & -q_{T1} & q_{T4} & -q_{T3} \\ q_{T1} & q_{T2} & q_{T3} & q_{T4} \end{bmatrix} \begin{bmatrix} q_1 \\ q_2 \\ q_3 \\ q_4 \end{bmatrix} \quad (16.)$$

Since, we do not require any precise attitude control in CCF-X axis, we disregard the error in this axis by setting $q_{E1} = 0$. By the definitions of quaternions we also have $q_{T1}^2 + q_{T2}^2 + q_{T3}^2 + q_{T4}^2 = 1$. Two more equations are then needed to obtain the dynamic reference attitude q_T.

In-track reference attitude

For the in-track direction the reference attitude takes the form as in Eq. (17) which gives us the two equations needed as $q_{T1} = q_{T4} = 0$.

$$q_T = [0 \quad q_{T2} \quad q_{T3} \quad 0]^T \quad (17.)$$

Solving for q_T, we obtain the following reference attitude vectors. Since we are concerned with both small and large deviations from reference attitude, the solution of Eq. (19) is unstable and thus we disregard it.

$$q_T = \begin{bmatrix} 0 & \frac{q_2}{\sqrt{q_2^2+q_3^2}} & \frac{q_3}{\sqrt{q_2^2+q_3^2}} & 0 \end{bmatrix}^T \quad (18.)$$

$$q_T = \begin{bmatrix} 0 & \frac{-q_2}{\sqrt{q_2^2+q_3^2}} & \frac{-q_3}{\sqrt{q_2^2+q_3^2}} & 0 \end{bmatrix}^T \quad (19.)$$

Anti-in-track reference attitude

Similar to the discussion for in-track direction, the anti-in-track direction dynamic reference attitude takes the form of Eq. (20), which infers that $q_{T2} = q_{T3} = 0$.

$$q_T = [q_{T1} \quad 0 \quad 0 \quad q_{T4}]^T \quad (20.)$$

Solving for q_T, we obtain two solution. Among them the stable solution for both small and large angle deviations is presented in Eq. (21).

$$q_T = \begin{bmatrix} \frac{q_1}{\sqrt{q_1^2+q_4^2}} & 0 & 0 & \frac{q_2}{\sqrt{q_1^2+q_4^2}} \end{bmatrix} \quad (21.)$$

4.2. Control laws

The attitude control law determines the required torque to meet the control problem. In the previous section, the two directions of interest (in-track and anti-in-track) have been translated into dynamic reference attitudes. In this section we present one linear control law (PD control) and one non-linear control law which is sliding mode control.

Proportional-derivative (PD) control

PD control is widely used for satellite's attitude control. Several variations of the PD control law are discussed in 11). A simple PD law is presented in Eq. (22). Application of PD control is quite common in the general 3-axes attitude control and we intend to evaluate it for this specific pointing requirement.

$$T_{PD} = -T_0\left(K_p[q_{E1} \quad q_{E2} \quad q_{E3}]^T + K_d[\omega_1 \quad \omega_2 \quad \omega_3]^T\right) \quad (22.)$$

where T_0 is the average thrust from the thrusters. The proportional gain is $K_p = diag(k_{p11}, k_{p22}, k_{p33})$ and the derivate gain is $K_d = diag(k_{d11}, k_{d22}, k_{d33})$.

Sliding mode control (SMC)

Sliding mode control is a discontinuous type of non-linear control. In this work, the sliding mode control laws are motivated from 12), but to capture the concept of dynamic reference attitude, the sliding variable has been modified. The sliding surface for SMC is defined by the Eq. (23)

$$S_v = \omega_{bo}^c + \Lambda_s[q_{E1} \quad q_{E2} \quad q_{E3}]^T \quad (23.)$$

where $\Lambda_s = diag(k_{s11}, k_{s22}, k_{s33})$ is the tunable parameter.

The control torque by sliding mode law has two parts. First part (T_{sm}), incorporates the non-linear dynamics of the system and keeps the system on the sliding manifold i.e. it makes sure that time derivative of sliding variable is zero ($\dot{S}_v = 0$). The second part (T_{sm}) brings the sliding variable to zero in a finite time. The two components of SMC torque are given by Eqs. (24) and (24).

$$T_{sv} = -\lambda_s sign(S_v) \quad (24)$$

$$T_{sm} = \omega_{bi}^c \times I_s\omega_{bi}^c - 3\omega_0^2(k_0^c \times I_s k_0^c) + \omega_0 I_s(i_o^c \times \omega_{bo}^c) - \tfrac{1}{2} I_s \Lambda_s(\omega_{bo}^c q_4 + \omega_{bo}^c \times q_{vec}) \quad (25)$$

where $q_{vec} = [q_1 \quad q_2 \quad q_3]^T$. As mentioned earlier, the total SMC torque is given by $T_{SMC} = T_{sv} + T_{sm}$.

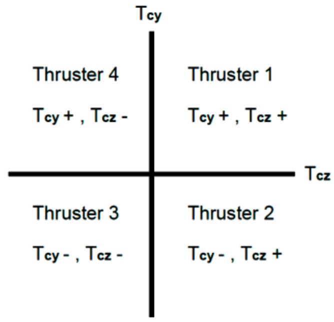

Fig. 2. Thruster control quadrants

4.3. Controller

The control law demands a specific control torque from the actuators. However, there are certain constraints to both the actuators types. The magnetic torquers cannot produce any arbitrary value of torques since their ability is depending on the instantaneous Earth's magnetic field. The thrusters can only produce torque couples of fixed strength according to Fig. 2 and hence, it is not possible to produce the exact demanded control torque.

When having only one thruster as ON (one quadrant action) during one simulation step, a simple but less accurate control torque is produced. However by the use of two thrusters (two quadrant action), one can come closer to the demanded torque.

Finally, it is also possible to combine the effects of thrusters and torquers to produce the demanded torque with the main intention to prolong the lifespan of the thrusters. It is important to note that thrusters cannot produce any torque in CCF-X axis. So when dividing the control torque between thrusters and torques, the torques must make an attempt to produce the entire control torque in CCF-X axis.

A simple split function for control torque demanded from torquers and thrusters is assumed and presented in Eqs. (26) and (27)

$$T_{thr} = \gamma[0 \quad T_{cy} \quad T_{cz}]^T \quad (26.)$$

$$T_{tor} = [T_{cx} \quad 0 \quad 0]^T + (1-\gamma)[0 \quad T_{cy} \quad T_{cz}]^T \quad (27.)$$

with γ being the split ratio. It is also important to note, that it is not desired to completely perform the attitude control with the torquers ($\gamma = 0$), since the thrust in the desired direction is required for orbit control. A dynamically adjustable split ratio, depending on the instantaneous mispointing, can further increase the controller's thrust efficiency.

5. Simulations

The simulation is developed in Matlab and Simulink environment. Based on the discussions in the previous sections, a variety of controllers are tested which will be presented in this section. It is important to mention that intensive efforts were not put in for tuning the controllers, therefore no strict performance comparison is performed.

Simulation experiments are performed with only magnetic control, only thruster control and a combination of them with both PD and SMC law. Both one and two quadrant actions are analyzed.

For all simulation experiments, one direction changes from in-track to anti-in-track directions is performed to check the stability and deterministic performance of the controller.

5.1. Magnetic control

An only magnetic control is implemented and tested with PD and SMC control law. Figure 3 shows the Magnetic control is not very efficient or stable when a direction change is demanded which is because the strength of the magnetic moment is not enough to cope with the disturbance torques, causing it to operate close to the unstable zone.

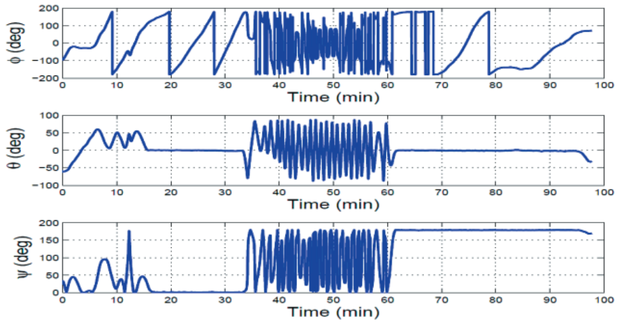

Fig. 3. Roll, Pitch and Yaw axes during attitude control for a change in direction from in-track to anti-in-track using only magnetic Control with SMC law

5.2. Thruster control

The thruster only control exhibits a tighter control as can be seen in Fig. 4 with PD control law. The system's reaction to the required large angle maneuver at 50 mins simulation time can smoothly be achieved within 150 seconds.

5.3. Combination of magnetic and thruster control

Since the thrusters have a limited lifespan, any complementary support to thrusters to achieve the attitude control while doing orbit correction is advantageous. The magnitude of torque produced by the torquers available for the UWE satellites is low compared to the proposed thrusters but it can be seen from the results in Table 2 that the torquers still help in reducing the average firings per minute (FPM) from the thrusters from 3017 to 2900.

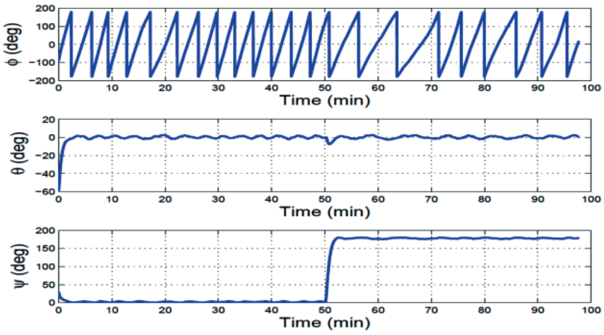

Fig. 4. Roll, Pitch and Yaw axes during attitude control for a change in direction from in-track to anti-in-track using only thrusters with PD law

The settling time and accuracy plot for the combination control with SMC law and two quadrant action controller is shown in Fig. 5 and 6. It can be concluded that tight attitude control can be obtained for UWE-4 by using the proposed nano-thrusters.

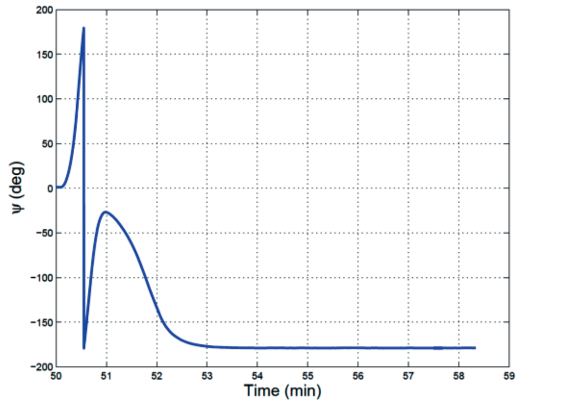

Fig. 5. Yaw angle settling time (160 s) for a change in direction from in-track to anti-in-track direction when using a combination of magnetic and thruster control with SMC law

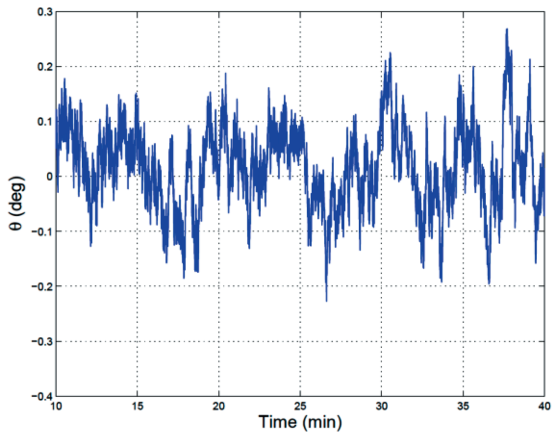

Fig. 6. Pitch angle settling accuracy ($\pm 2.5^0$) for a change in direction from in-track to anti-in-track direction when using a combination of magnetic and thruster control with SMC law

6. Conclusions

Formation flying satellites gain attention and due to ongoing miniaturization efforts, also in the electric propulsion domain, CubeSats become suitable platforms for such missions. UWE-4 will demonstrate the use of electric propulsion in the 1 unit CubeSat form factor for orbit and attitude control.

For the sake of orbit correction or maneuvering, the CubeSat shall be able to change between in-track and anti-in-track direction with the need for frequent maneuvers. Limited attitude actuation present along the thrust axis motivated the search for dynamic target quaternions. The two dynamic attitude target equations obtained for each direction, also aim for attitude stabilization in X-axis which in turn helps in better attitude control in the Y and Z axes.

In this contribution, the main focus of study lays on the attitude control for the purpose of orbit control, i.e. to enable frequent large angle maneuvers. With the presented tuning of the two control laws, the sliding mode control performs better than the PD control law in terms of the stability of the X-axis and the attitude accuracy in terms of settling interval. This can be explained by the fact that the PD law has no knowledge of the plant dynamics while the sliding mode control law compensates for the dynamics. It can be clearly observed from Tab. 2 that the higher attitude accuracy algorithm is demanding a higher utilization of the thrusters (i.e. firings per minute, FPM), which is not an undesired effect since thrust is primarily delivered in the desired direction. Both controller were found to be stable but it is important to mention that global stability is not guaranteed if the saturation limit on thruster firing frequency is increased. Detailed study of the unstable zones for attitude control is the future work.

While the UWE-4 mission is being prepared at the University of Wuerzburg, the Zentrum fuer Telematik, Germany, develops in parallel the formation flying demonstrator mission NetSat. Future developments of the platform therefore target inter-satellite communication, orbit determination, formation control, and autonomous mission planning.

Acknowledgments

The authors appreciated the support for UWE-3 by the German national space agency DLR (Raumfahrt-Agentur des Deutschen Zentrums für Luft- und Raumfahrt e.V.) by funding from the Federal Ministry of Economics and Technology by approval from German Parliament with reference 50 RU 0901 as well as the European Research Council advanced grant "NetSat".

References

1) M. Schmidt and K. Schilling, "Formation Flying Techniques for Pico-Satellites", *6th International Workshop on Satellite Constellation and Formation Flying*, IWSCFF-Paper-2010-3-5, 2010.
2) S. Busch, P. Bangert, S. Dombrovski, K. Schilling, "UWE-3, In-Orbit Performance and Lessons Learned of a Modular and Flexible Satellite Bus for Future Picosatellite Formations", *65th International Astronautical Congress*, Toronto, 2014
3) S. Busch, P. Bangert, K. Schilling, "Attitude Control Demonstration for Pico-Satellite Formation Flying by UWE-3", *Proceedings of Small Satellites Systems and Services - The 4S Symposium*, Mallorca, 2014
4) P. Bangert, S. Busch, K. Schilling, "Performance Characteristics of the UWE-3 Miniature Attitude Determination and Control system", *2nd IAA Conference on Dynamics and Control of Space Systems (DYCOSS)*, Rome, 2014
5) J. Mueller, R. Hofer, and J. Ziemer, "Survey of propulsion technologies applicable to cubesats," Jet Propulsion Laboratory, California Institute of Technology, Tech. Rep., 2010
6) M. J. Sidi, *Spacecraft Dynamics and Control*, M. J. Rycroft and R. F. Stengel, Eds. Cambridge University Press, 1997
7) C. Roithmayr, "Contributions of spherical harmonics to magnetic and gravitational fields," NASA Johnson Space Center, Tech. Rep., 1996
8) I. Kronhaus, K. Schilling, S. Jayakumar, and A. Kramer, "Design of the UWE-4 picosatellite orbit control system using vacuum-arc-thrusters," in *33rd International Electric Propulsion Conference*, 2014.
9) F. Reichel, P. Bangert, S. Busch, K. Ravandoor, and K. Schilling, "The attitude determination and control system of the picosatellite uwe-3," in *19th IFAC Symposium on Automatic Control in Aerospace*, 2013.
10) J. Li, M. Post, T. Wright, and R. Lee, "Design of attitude control systems for cubesat-class nanosatellite," *Journal of Control Science and Engineering*, 2013
11) B. Wie and P. M. Barbat, "Quaternion feedback for spacecraft large angle maneuvers," *Journal of Guidance Control and Dynamics*, vol. 8, pp. 360–365, 1985
12) R. Wisniewski, "Satellite attitude control using only electromagnetic actuation", Ph.D. dissertation, Department of Control Engineering, Aalborg University, 1996

Table 2. Performance with different simulated scenario

	Control law and Thruster action	Settling Interval	Settling Time	Avg. FPM
Magnetic Control	PD	uncontrolled		
	SMC	Y: ±1.2° Z:1.5° ± 1.2°	28 min	
Thruster Control	PD - One quad	Y: ±2.5° Z:2 ± 2°	150 s	476
	SMC - One quad	Y: ±0.3° Z:1.2 ± 0.3°	240 s	3017
Combination of Magnetic and Thruster Control	PD - One quad	Y: ±2.0° Z:2 ± 3.5°	120 s	215
	PD - Two quad	Y: ±6.0° Z:±8.0°	90 s	78
	SMC - One quad	Y: ±0.25° Z:1.25 ± 0.2°	200 s	2938.4
	SMC - Two quad	Y: ±0.25° Z:1.25 ± 0.2°	160 s	2900.1